Bioorganic Chemistry 83 (2019) 367–379

Contents lists available at ScienceDirect

Bioorganic Chemistry

journal homepage: www.elsevier.com/locate/bioorg

Novel 4-(3-phenylpropionamido), 4-(2-phenoxyacetamido) and 4-(cinnamamido) substituted benzamides bearing the pyrazole or indazole nucleus: synthesis, biological evaluation and mechanism of action

Demetrio Raffa[a,1,*], Antonella D'Anneo[b,1], Fabiana Plescia[a,*], Giuseppe Daidone[a], Marianna Lauricella[c,2], Benedetta Maggio[a,2]

[a] University of Palermo, Department of Biological, Chemical and Pharmaceutical Sciences and Technologies (STEBICEF), Medicinal Chemistry and Pharmaceutical Technologies, Via Archirafi 32, 90123 Palermo, Italy
[b] University of Palermo, Department of Biological, Chemical and Pharmaceutical Sciences and Technologies (STEBICEF), Laboratory of Biochemistry, Via del Vespro 129, 90127 Palermo, Italy
[c] University of Palermo, Department of Experimental Biomedicine and Clinical Neurosciences, Laboratory of Biochemistry, Via del Vespro 129, 90127 Palermo, Italy

ARTICLE INFO

Keywords:
2-(3-phenylpropanamido)benzamides
2-(2-phenoxyacetamido)benzamides
2-cinnamamidobenzamides
P53
TRAIL-receptors
Apoptosis

ABSTRACT

Based on some common structural features of known compounds interfering with p53 pathways and our previously synthesized benzamides, we synthesized new ethyl 5-(4-substituted benzamido)-1-phenyl-1H-pyrazole-4-carboxylates **26a-c**, ethyl 5-(4-substituted benzamido)-1-(pyridin-2-yl)-1H-pyrazole-4-carboxylates **27a-c** and N-(1H-indazol-6-yl)-4-substituted benzamides **31a,b** bearing in the 4 position of the benzamido moiety the 2-phenylpropanamido or 2-phenoxyacetamido or cinnamamido groups. A preliminary test to evaluate the antiproliferative activity against human lung carcinoma H292 cells highlighted how compound **26c** showed the best activity. This last was therefore selected for further studies with the aim to find the mechanism of action. Compound **26c** induces intrinsic apoptotic pathway by activating p53 and is also able to activate TRAIL-inducing death pathway by promoting increase of DR4 and DR5 death receptors, downregulation of c-FLIP$_L$ and caspase-8 activation.

1. Introduction

The tumor suppressor p53 is a highly regulated transcription factor that plays a fundamental role in preventing tumorigenesis [1]. In normal cells p53 levels are tightly controlled via the E3 ubiquitin ligase MDM2, that binds p53 promoting its ubiquitination and proteasomal degradation [2]. This represents a regulatory mechanism to maintain in normal cells low levels of p53 preventing aberrant apoptosis. In response to DNA damage or other cellular stress signals p53 is activated and induces up- or down regulation of a variety of genes involved in cell cycle arrest [1], DNA repair [3], senescence [4], or apoptosis [5]. The activity and cellular levels of p53 are regulated through post-transcriptional and post-translational mechanisms, including phosphorylation, acetylation, sumoylation, and methylation [2,6].

p53 function is compromised in almost 50% of human cancers through inactivating mutations in p53 gene [7]. In cancers in which the p53 gene is not mutated, the function of the p53 is often inhibited through other mechanisms, including increased expression of MDM2 or inactivation of the tumor suppressor protein p14/ARF [8]. Several strategies can be undertaken to restore the altered p53 pathways in tumor cells such as reactivation of structural stability, reactivation of p53 transcriptional activity, inhibition of p53/MDM2 interaction [7], by small molecules [9]. Sendermetan **1**, SJ-172550 **2** and RO-2443 **3** [9], C646 **4** [10], BIRB-796 **5** [11,12], HZ00 **6** [13], Chidamide (Tucidinostat) **7** [14], and (MS-27–275) **8** [15], Tenovin-1 **9** [16], Tenovin-6 **10** [16], Sorafenib **11**[17] and compound **12** [18] (Fig. 1), are some examples of active molecules which are able to restore p53 activity with different mechanisms.

Despite their different mechanisms of action, some structural features are common to them. In particular, the molecules have the ability to assume several conformations due to the free rotation around the several sigma bonds in the structure; superimposition of the staggered

* Corresponding authors.
E-mail addresses: demetrio.raffa@unipa.it (D. Raffa), fabiana.plescia@unipa.it (F. Plescia).
[1] These authors contributed equally to this work.
[2] These authors contributed equally to this work.

https://doi.org/10.1016/j.bioorg.2018.10.055
Received 17 August 2018; Received in revised form 3 October 2018; Accepted 27 October 2018
Available online 29 October 2018
0045-2068/

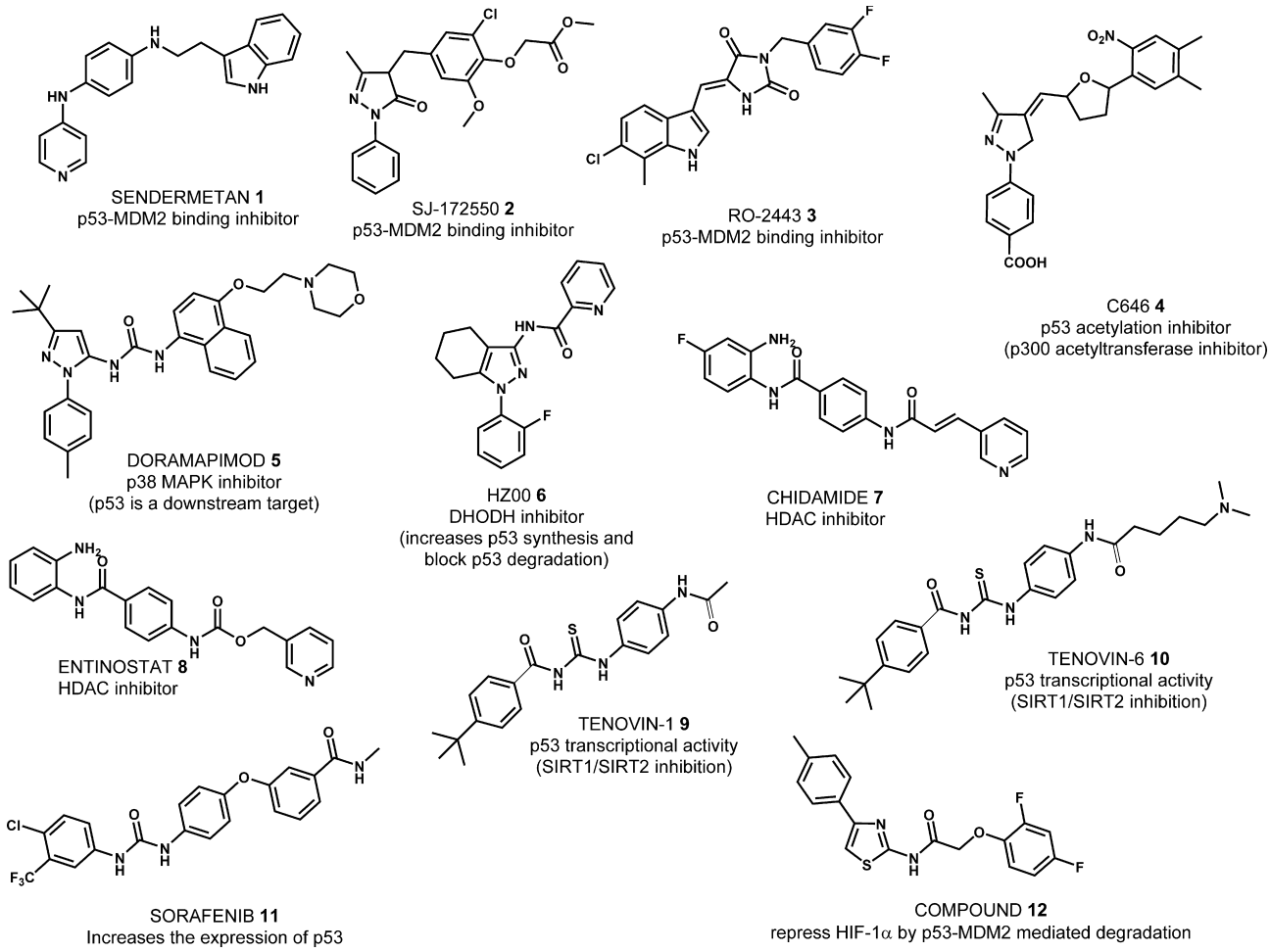

Fig. 1. Examples of compounds interfering with p53 pathways.

conformation of these molecules shows a chain length ranging between 11 and 20 Å. All the structures present two or more electronegative atoms able to form hydrogen bonds. Finally, an overview of the structures in Fig. 1 shows the presence of some typical moieties such as: pyrazole, ethylene, vinylene and phenoxyacetamido (Fig. 2).

In the last decade we have dealt with studying the antitumor activity of several new compounds trying to elucidate the mechanisms of action underlying their activity [19–24]. We also studied the

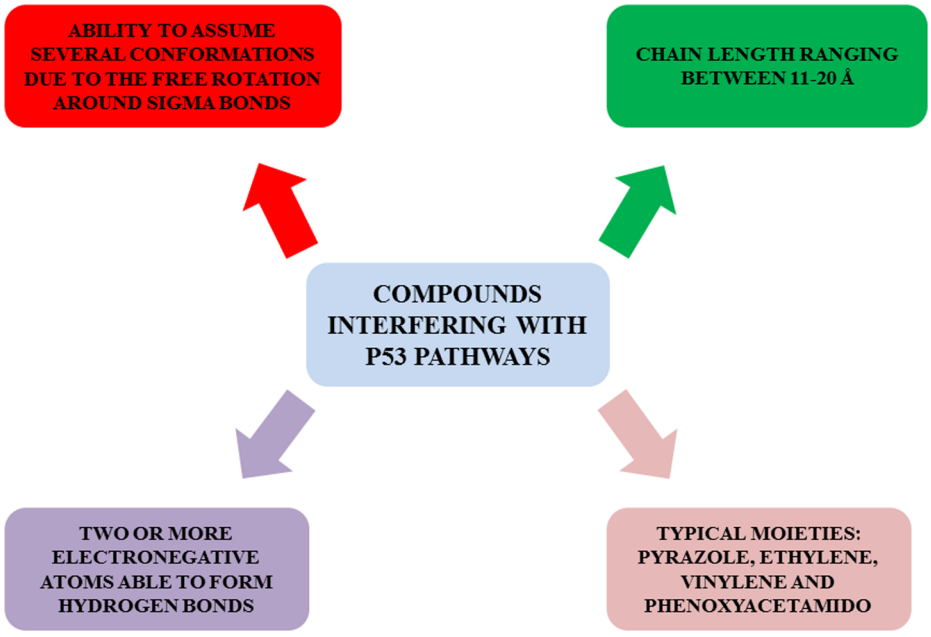

Fig. 2. Structural common features of compounds interfering with p53 pathways.

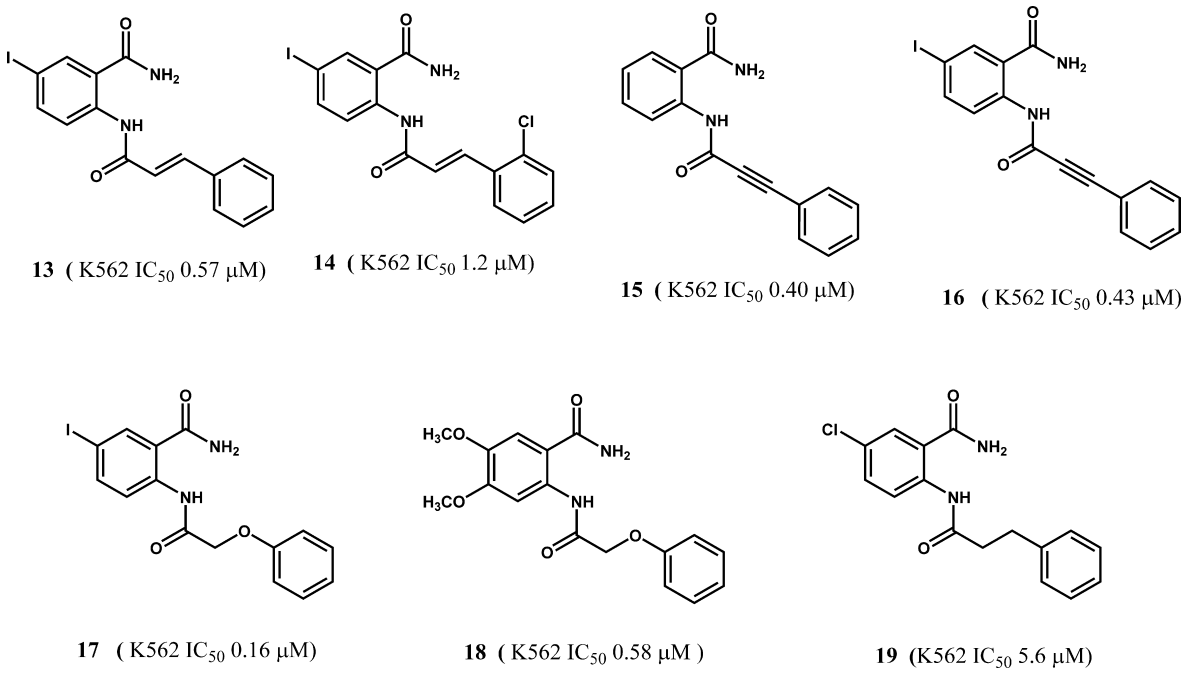

Fig. 3. Previously synthesized anthranilamides **13–19**.

relationship between the mechanism of action and the scaffold bound to the benzamido moiety of some anthranilamide derivatives (Fig. 3, compounds **13–19**) [25–28].

On that basis, in this paper, our strategy was to make some structural modification on our anthranilamides in order to make new molecules having the common features of compounds interfering with p53 pathways (Fig. 4).

In particular, first we have selected anthranilamides bearing the phenylpropanamido, cinnamamido and 2-phenoxyacetamido moieties then, we have moved the carboxyamido group from the ortho to the

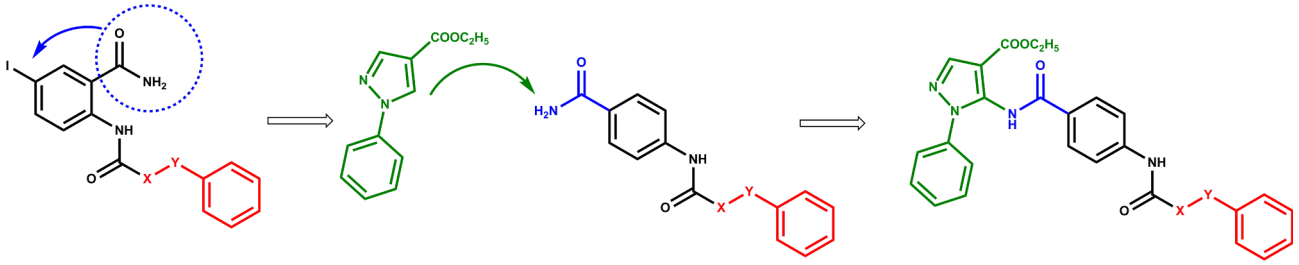

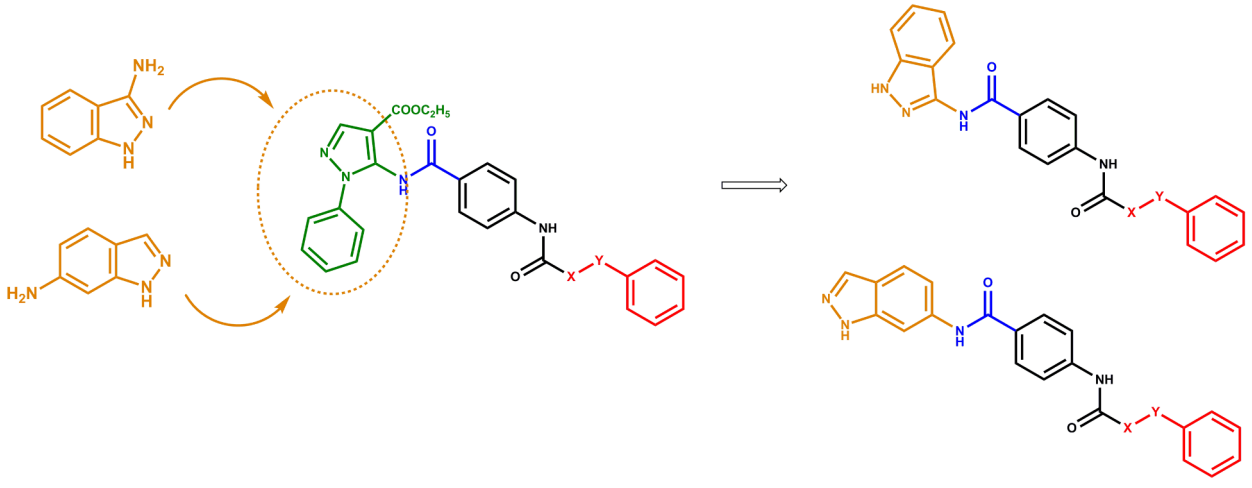

Fig. 4. Structural modification on anthranilamides.

para position. Also, we have lengthened the molecules by adding an *N*-phenylpyrazole nucleus presents in some compounds interfering with p53 pathways (Fig. 4).

Finally, the biological profile of derivatives containing the indazole nucleus, a fused bicyclic pyrazole, instead of *N*-phenylpyrazole was also investigated (Fig. 4).

The new synthesized molecules were evaluated both for their antiproliferative activity and toxicity on both human normal and cancer cells. Compounds that showed good activity were further studied to ascertain if the aforementioned structural modification could make them able to interfere with p53 pathways. Finally, the best active compound was used to study in deep the mechanism of action through which they exert their effects.

2. Results and discussion

2.1. Chemistry

A series of pyrazole-4-carboxylates **26a-c**, **27a-c** and **31a,b** were synthesized as described in Schemes 1 and 2. Crude acyl chlorides **25a-c** were obtained by refluxing the appropriate acids **24a-c** with thionyl chloride. The ethyl 5-(4-nitrobenzamido)-1H-pyrazole-4-carboxylates **22a**,**b** were synthesized by refluxing the 4-nitrobenzoyl chloride **20** with the 1H-pyrazole-4-carboxylates **21a**,**b** in acetonitrile for 8 h (Scheme 1). Compounds **22a,b** were therefore transformed by hydrogenation in presence of palladium on charcoal to give the corresponding amines **23a,b**. Finally, the reaction of amines **23a,b** with acyl chlorides **25a-c**, gave the expected derivatives **26a-c** and **27a-c**.

Furthermore, as reported in Scheme 2, the reaction of the 4-nitrobenzoyl chloride **20** with 6-aminoindazole **28** in pyridine at 0–5 °C gave the nitrobenzamide **29** which, in turn, was transformed by hydrogenation in presence of palladium on charcoal to give the 4-aminobenzamide **30**. Derivatives **31a,b** were finally obtained by reacting, in pyridine at 0–5 °C, the compound **30** and the acyl chlorides **25a,b**.

Attempt to obtain the 4-nitrobenzamide **33** with the same way, failed. The reaction of the 4-nitrobenzoyl chloride **20** with 1H-indazol-3-amine **32** gave the unexpected derivative **34** instead of the compound **33** (Scheme 3).

2.2. Biology

2.2.1. Benzamides exerts exert antiproliferative effects on human H292 lung mucoepidermoid carcinoma cells

Synthesized benzamides **26a-c**, **27a-c** and **31a,b** were initially tested *in vitro* for their antiproliferative activity against the human lung mucoepidermoid carcinoma H292 cell line. The percent growth inhibition at a screening concentration of 10 μM at 48 h of treatment for compounds are shown in Table 1.

The antiproliferative effects of the benzamides were compared with that exerted in the same cells by SAHA (Vorinostat). SAHA is, a deacetylase inhibitor which has been shown to induce apoptosis in different tumor cell lines by activating p53 [29] and that is currently employed for clinical application [30]. Compounds **26a**, **26c**, **27a**, and **27c**, which showed the greatest efficacy in the preliminary experiments, have been the subject of further studies. To this end, H292 cells were treated with increasing concentrations of each compound (within

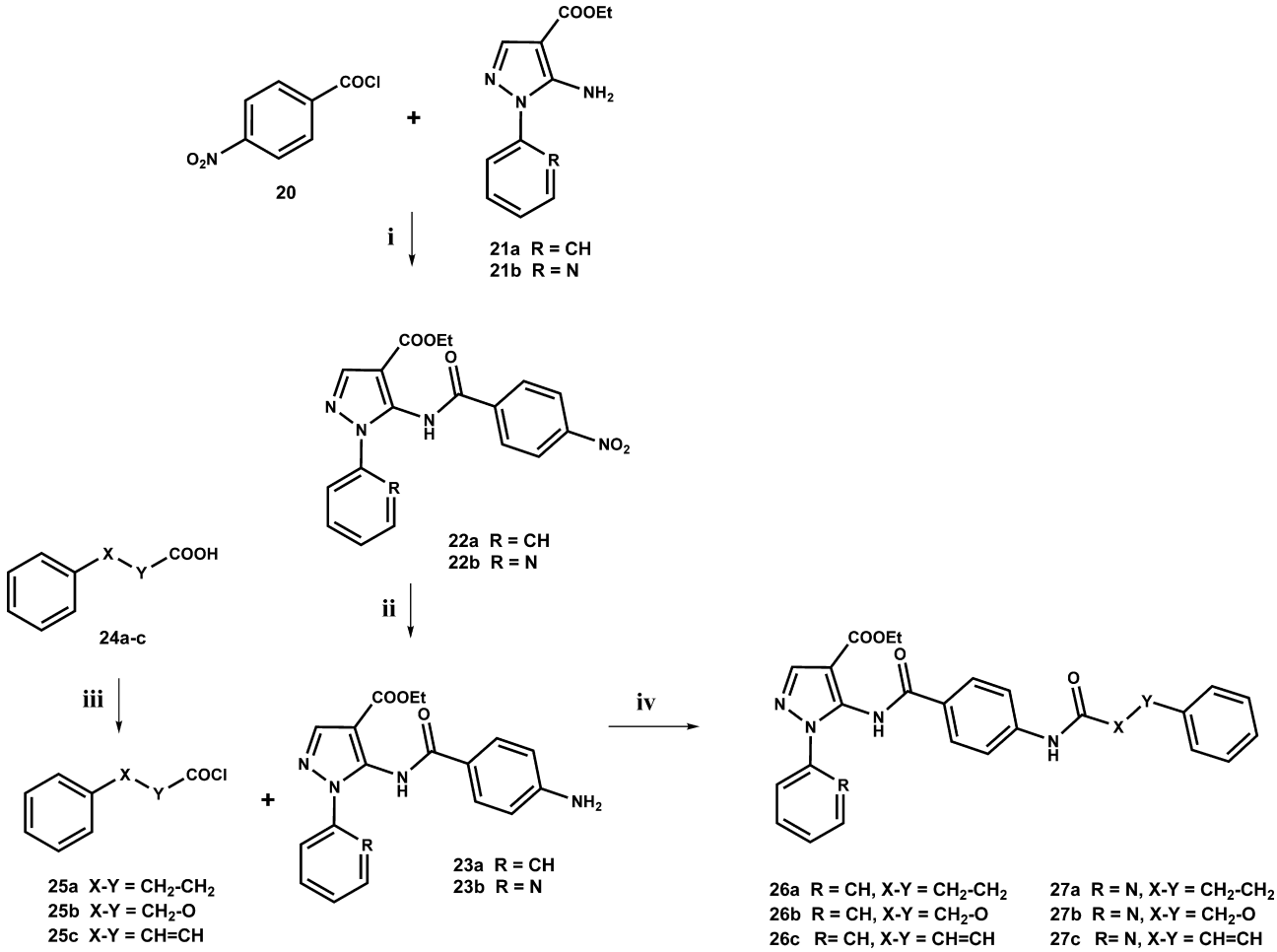

Scheme 1. Synthetic pathway to obtain compounds **26** and **27**: (i) acetonitrile, reflux, 8 h; (ii) ethanol, H_2, Pd-C, 20 h; (iii) thionyl chloride, reflux, 5 h; (iv) acetonitrile, reflux, 8 h.

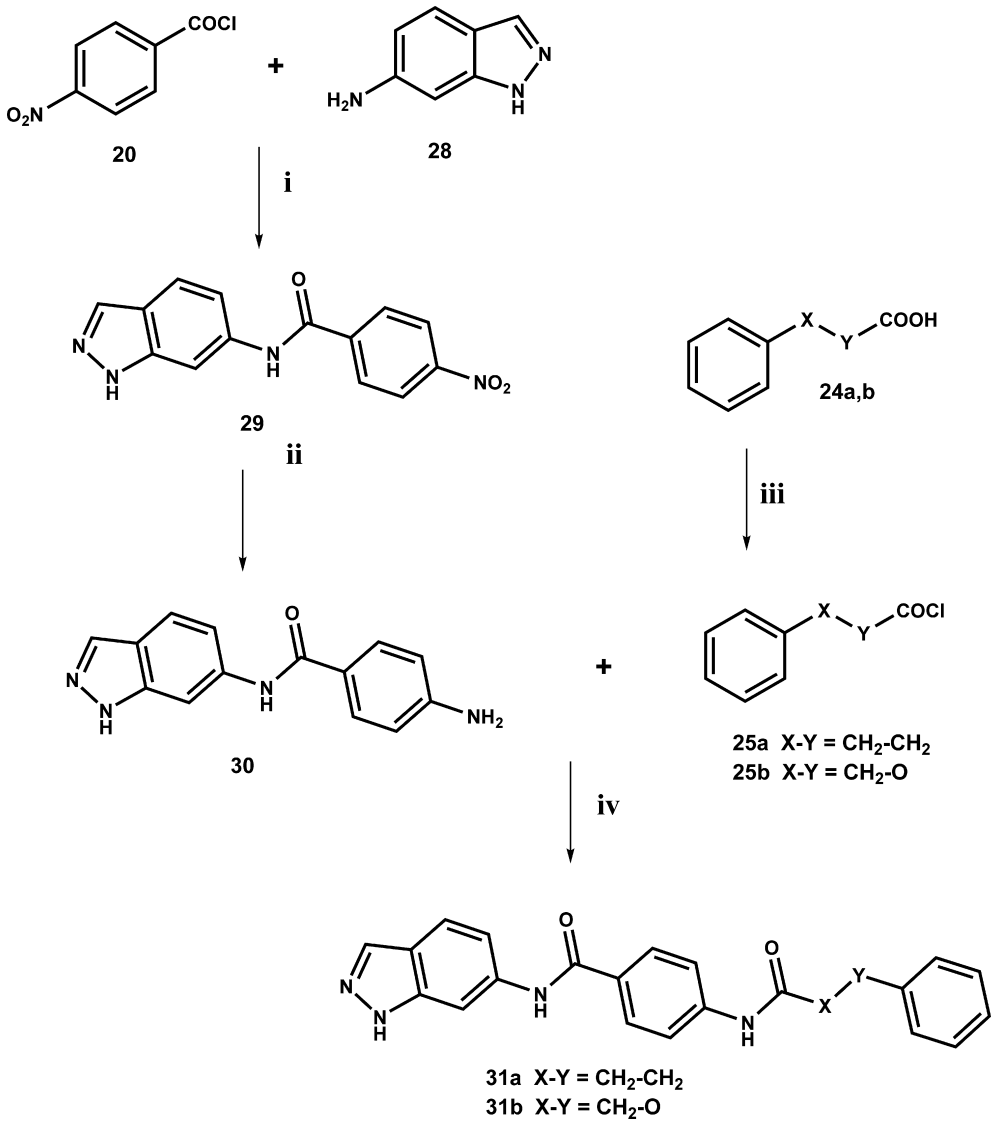

Scheme 2. Synthetic pathway to obtain compounds **31**: (i) pyridine, 0–5 °C, 24 h; (ii) ethanol, H_2, Pd-C, 20 h; (iii) thionyl chloride, reflux, 5 h; (iv) pyridine, 0–5 °C, 24 h.

the range of 5–40 μM) for 48 h and the viability was evaluated by MTT assay as reported in Methods. Fig. 5A shows that **26a**, **27a** and **27c** did not exert a significant cytotoxic effect on H292 cells even at higher used concentration. In fact, their IC50 at 48 h of treatment were greater than 50 μM. Instead, **26c** markedly reduced the H292 cell viability compared with control cells in a dose-dependent manner with an IC50 of 5 μM at 48 h of treatment. Interestingly, **26c** exerted on H292 cells an anti-proliferative effect similar to SAHA, which exhibited on H292 an IC50 of 5 μM at 48 h of treatment (not shown). This data is in accordance with our previous results obtained in H292 cells [31].

The activity of **26c**, which turned out to be the most active, was also evaluated on HDFα, a normal human fibroblast cell line. Interestingly, the effect of the compound was less pronounced than in H292 cells (IC50 of 20 μM at 48 h of treatment), thus suggesting that this compound may have limited toxicity in vivo at doses that would limit tumor growth (Fig. 5B).

Having demonstrated growth-inhibiting effect of **26c**, we next examined its effect on colony formation by a clonogenic assay. This procedure determines the ability of a cell to indefinitely proliferate, thereby retaining its ability to form a large colony or a clone also after the treatment with an antitumor compound. To this end, H292 cells were plated with and without the addition of increasing doses of **26c** and untreated and treated cells were maintained in culture for additional 10 days to allow formation of colonies. The results demonstrated that **26c** suppressed the colony formation in H292 cells in a dose-dependent manner when compared with the untreated groups (Fig. 5C).

2.2.2. *Apoptotic effects of compound **26c** on H292 cells*

To determine whether **26c** inhibited cell growth by inducing apoptosis, H292 cells were treated with increasing concentrations of the compound (1–5 μM) for different times and stained with AO/EB as reported in Methods. The results shown in Fig. 6 revealed that untreated cells appeared viable with bright green nuclei, whereas cells treated with **26c** showed nuclear condensation and DNA fragmentation, characteristic signs of the apoptotic cell death. The effect appeared after 24 h of treatment and increased at 48 h.

2.2.3. *26c treatment induces the activation of intrinsic and extrinsic apoptotic pathways on H292 cells*

Then, flow cytometric analyses with propidium iodide (PI) staining of DNA were performed to investigate the distribution of cells in the different phases of the cell cycle. These studies showed that **26c** increased the amount of cells in subG0/G1 phase, characteristic of apoptotic cells with fragmented DNA. As shown in Fig. 7, the

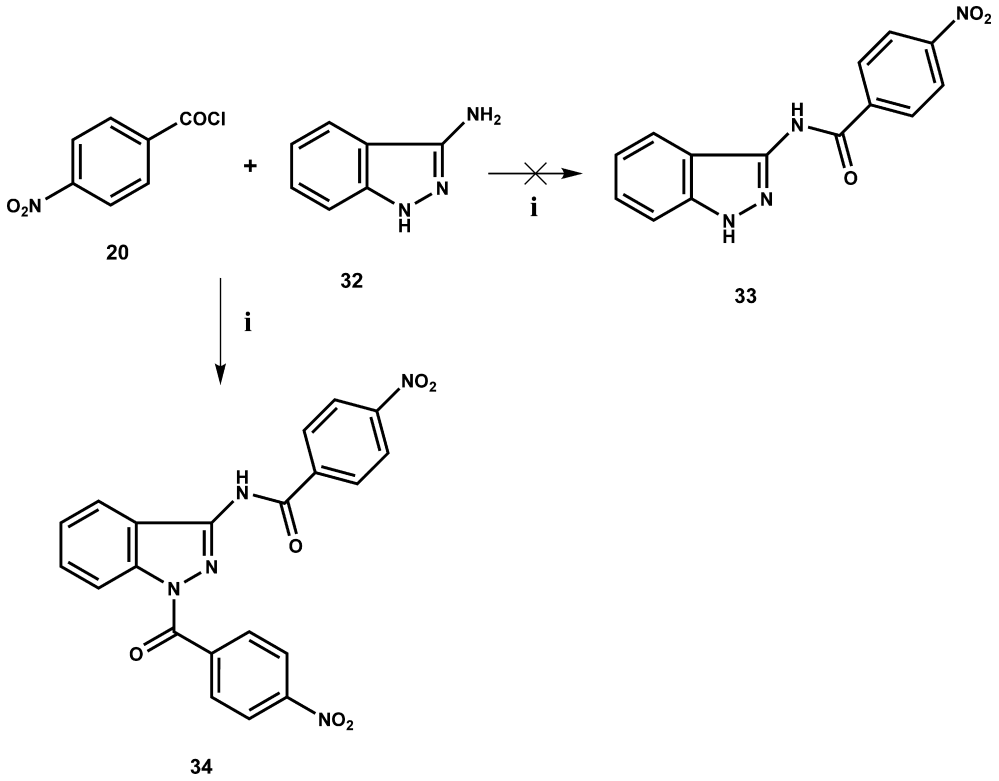

Scheme 3. Synthetic pathway to obtain compounds **34**: (i) pyridine, 0–5 °C, 24 h..

Table 1
Percent growth inhibition obtained with the H292 cell line with compounds at 10 μM at 48 h.

Comp.	H292 (10 μM)
26a	15
26b	11
26c	60
27a	20
27b	12
27c	25
31a	ns
31b	14
SAHA	60

ns not significant (% inhibition < 10%).

proportion of H292 cells in subG0/G1 phase increased from 0.5% in control cells to 22.9% in 5 μM **26c**-treated cells at 48 h. This effect was time-dependent, in fact prolonging the time of treatment to 72 h the percentage of **26c**-treated cells in subGo/G1 reached 30.5%.

p53 is a master regulator of the intrinsic apoptotic pathway in response to DNA damage or different kind of cellular stress [32]. To explore the ability of **26c** to induce p53 in lung cancer cells, the level of the protein was analysed by western blotting (Fig. 8A). Densitometric quantification of bands obtained in repeated experiments showed that **26c** increased in H292 cells the levels of p53 already after 24 h of treatment. In particular, in comparison with the control, cells treated with 5 μM **26c** showed an increase in the levels of p53 by 4.6-fold and 2.8-fold after 24 and 48 h, respectively.

It has been reported that p53 undergoes to different post-translational modifications for its regulation and activation [1]. Acetylation of p53 at carboxyl-terminal lysine residues is an important reversible enzymatic change that occurs in response to DNA damage and genotoxic stress [29]. This event has been shown to enhance the p53 transcriptional activity associated with cell cycle arrest and apoptosis [33]. Our data showed that in H292 cells **26c** treatment induced an increase of the acetylated form of p53 (Fig. 8A), thus suggesting the activation of the transcription factor. The effect was more pronounced after 24 h of treatment with 5 μM **26c** (increase of 3.2-fold respect to the control).

It is known that p53 regulates the expression of Bcl-2 family members which are involved in the control of mitochondrial membrane integrity [5]. In particular p53 up-regulates the levels of pro-apoptotic members Bax and PUMA, while down-regulates the expression of the anti-apoptotic ones such as Bcl-2 and Bcl-XL [34]. These events favor mitochondrial membrane potential dissipation and activation of apoptosis. Our data shown in Fig. 8B demonstrated that H292 cells exposed to 5 μM **26c** exhibited a time-dependent decrease in Bcl-2 expression compared with control cells. The decrease of Bcl-2 level was evident at 48 h of treatment, differently from the increase of p53 and its acetylated form. This different temporal effect is related to the fact that p53 activation is an early event of intrinsic apoptotic pathway, which then regulates Bcl-2 decrease.

TRAIL (Apo2L), a member of the TNF superfamily, is involved in the activation of apoptotic extrinsic pathway in a number of tumor cell lines but is ineffective in the majority of normal ones [29,35]. Binding of TRAIL to its receptors DR4 (TRAILR1) or DR5 (TRAILR2) results in the trimerization of the receptors with the production of the death-inducing signalling complex (DISC). Within this complex, pro-caspase-8 is activated by autoproteolytic cleavage with the consequent activation of effector caspases, such as caspase-3 and caspase-6, and induction of apoptosis [36].

Activation of caspases-8 can be inhibited by the cellular c-FLIP$_L$, which prevents the recruitment of the pro-caspase into the DISC complex. To ascertain whether **26c** is involved in the activation of TRAIL-induced apoptosis, we performed western blotting analyses to evaluate the effects of the compound on TRAIL receptors, caspase-8 and c-FLIP$_L$. Our results demonstrated that H292 cells exhibit both DR4 and DR5 receptors and that the level of these death receptors was up-regulated by **26c** treatment (Fig. 9A and B). The effect was more pronounced for DR4, whose levels increased by 2.5 fold in cells treated with 5 μM **26c** for 48 h respect to the control (Fig. 9A). Our results also demonstrated

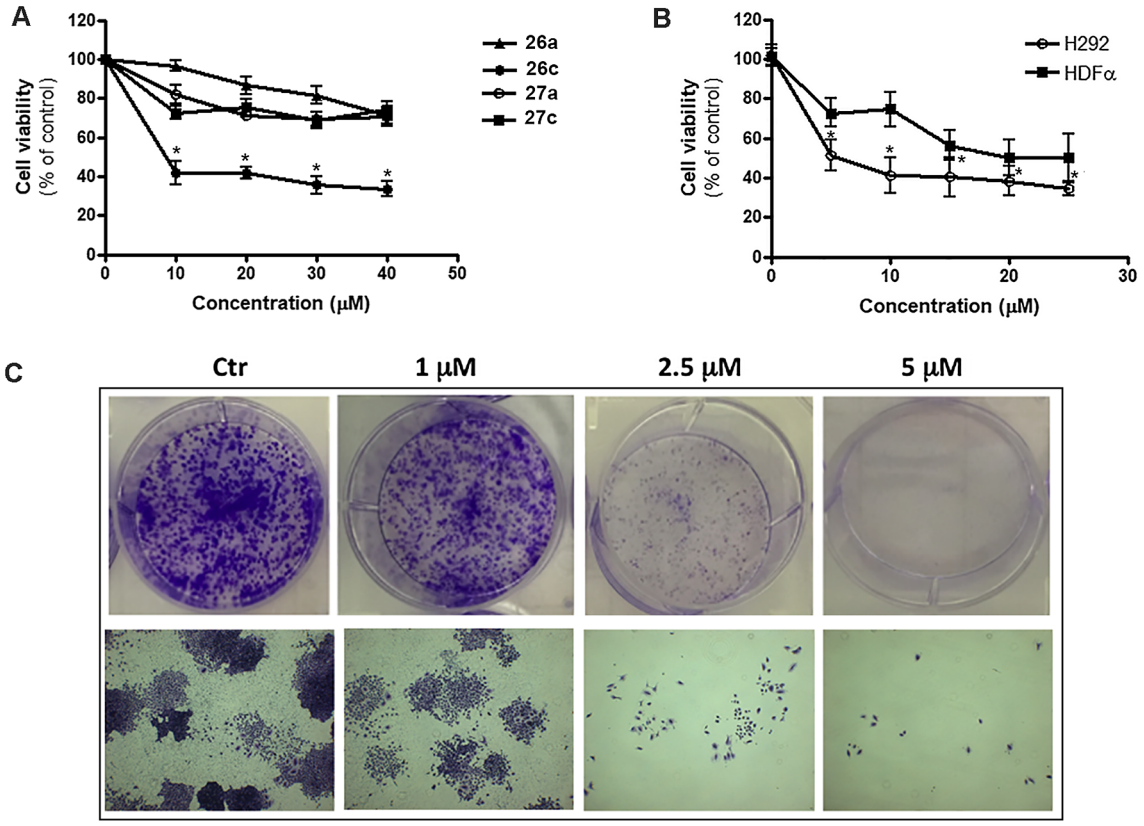

Fig. 5. Effects of benzamides on H292 cell viability and colony generation ability. H292 cells (5×10^3) were incubated in the presence of various doses of **26a**, **26c**, **27a**, and **27c** for 48 h, (B) The dose dependent effect of **26c** compound evaluated in both human lung mucoepidermoid carcinoma H292 cells and normal human HDFα cells at 48 h of treatment. Then the cytotoxic effect was determined by MTT assay as described in Section 4.2.1. Values are the means of three independent experiments ± S.E. (*) $p < 0.05$ compared to the untreated sample. (C) Effect of compound **26c** on colony generation ability of H292 cells. Clonogenic assay was performed seeding a single cell suspension (200 cells) in 6-well plates and after 48 h the treatment was performed with different doses of compounds. The ability of cells to generate colonies was evaluated after 10 days as reported in Methods. The number of colonies for each condition is reported in the upper panel of the figure, whereas the number of cells for each colony is reported in the lower panel.

that **26c** reduced the levels of c-FLIP$_L$ as well as decreased the levels of pro-caspase-8, thus suggesting the activation of the protease (Fig. 9A).

3. Conclusion

Our data demonstrated that **26c** exerted cytotoxic effects in H292 cells, a human lung carcinoma cell line with an IC_{50} at 48 h of 5 μM. The cytotoxic effect of the compound is due to the activation of apoptosis, as shown by AO/EB staining and flow cytometric analyses. In particular our data provided evidence that **26c** activated both intrinsic and extrinsic apoptotic pathways. In fact, **26c** increased p53 level as well as its acetylated form, which can be responsible for the decrease in Bcl-2 level. Furthermore, **26c** activated TRAIL-inducing apoptosis by up-regulating DR4 and DR5 and down-regulating c-FLIP$_L$ with the

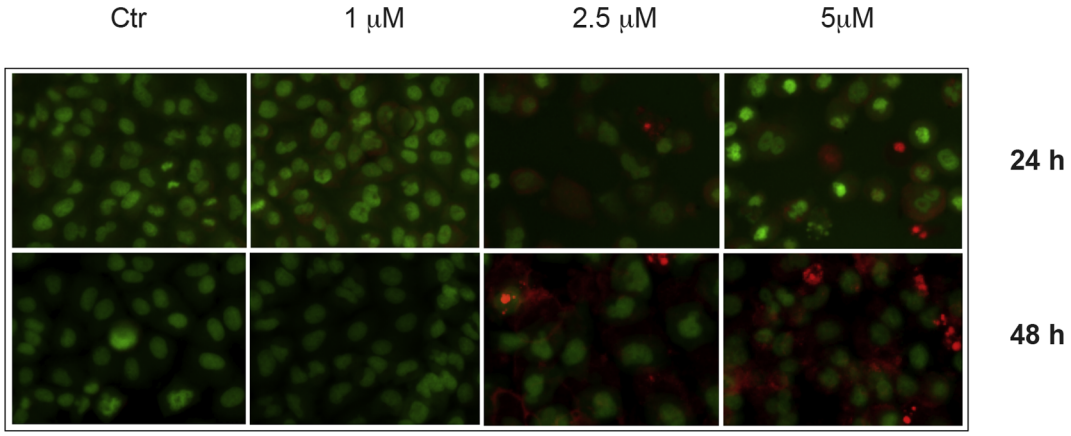

Fig. 6. Apoptotic effect induced by **26c** in human lung mucoepidermoid carcinoma H292 cells. The figure describes the effects of **26c** treatment on H292 cell morphology analyzed by fluorescence microscopy, after acridine orange/ethidium bromide double staining, as described in Sections 4.2.1 and 2. Three different visual fields were examined for each condition. Microphotographs were taken at a magnification of 200×. Results are representative of three independent experiments.

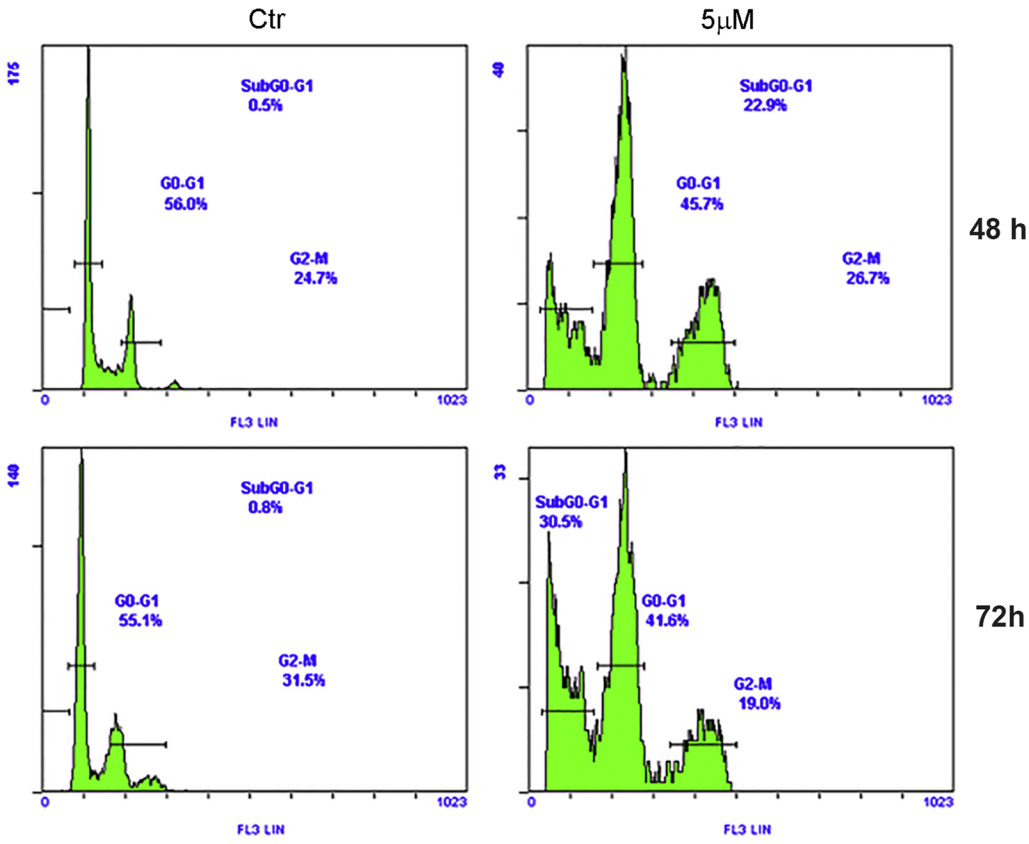

Fig. 7. Compound **26c** effects on H292 cell cycle distribution. Human lung mucoepidermoid carcinoma H292 cells were treated with **26c** for the indicated times, then the DNA content was evaluated by flow cytometry after propidium iodide staining as reported in Section 4.2.1. The percentage of cells in the different cell cycle phases was calculated by Expo 32 software.

consequent activation of caspase-8. The increase of TRAIL death receptors may be also a consequence of p53 activation, because it has been reported that DR4 and DR5 are transcriptional targets of p53 [37]. Moreover, TRAIL-induced apoptotic signaling can also contribute, through Bid activation, to down-regulate Bcl-2 levels [34]. A possible schematic model of **26c** cytotoxic effects in H292 is reported in Fig. 10.

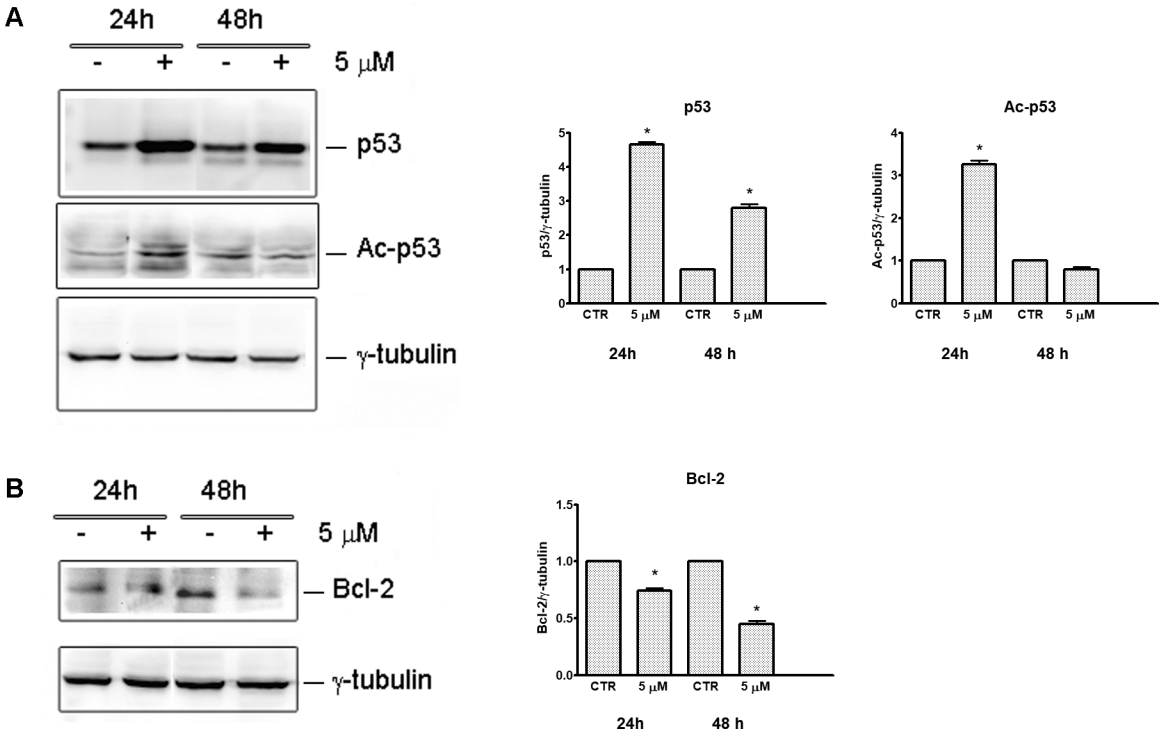

Fig. 8. Western blotting of p53, acetylated p53 (Ac-p53) and Bcl-2 in **26c** -treated H292 cells. All analyses were performed after 24 and 48 h of treatment with **26c** compound. The correct protein loading was ascertained by immunoblotting for γ-tubulin. Representative blots of three independent experiments and densitometric analysis are shown. (*) $p < 0.05$ compared to the untreated sample.

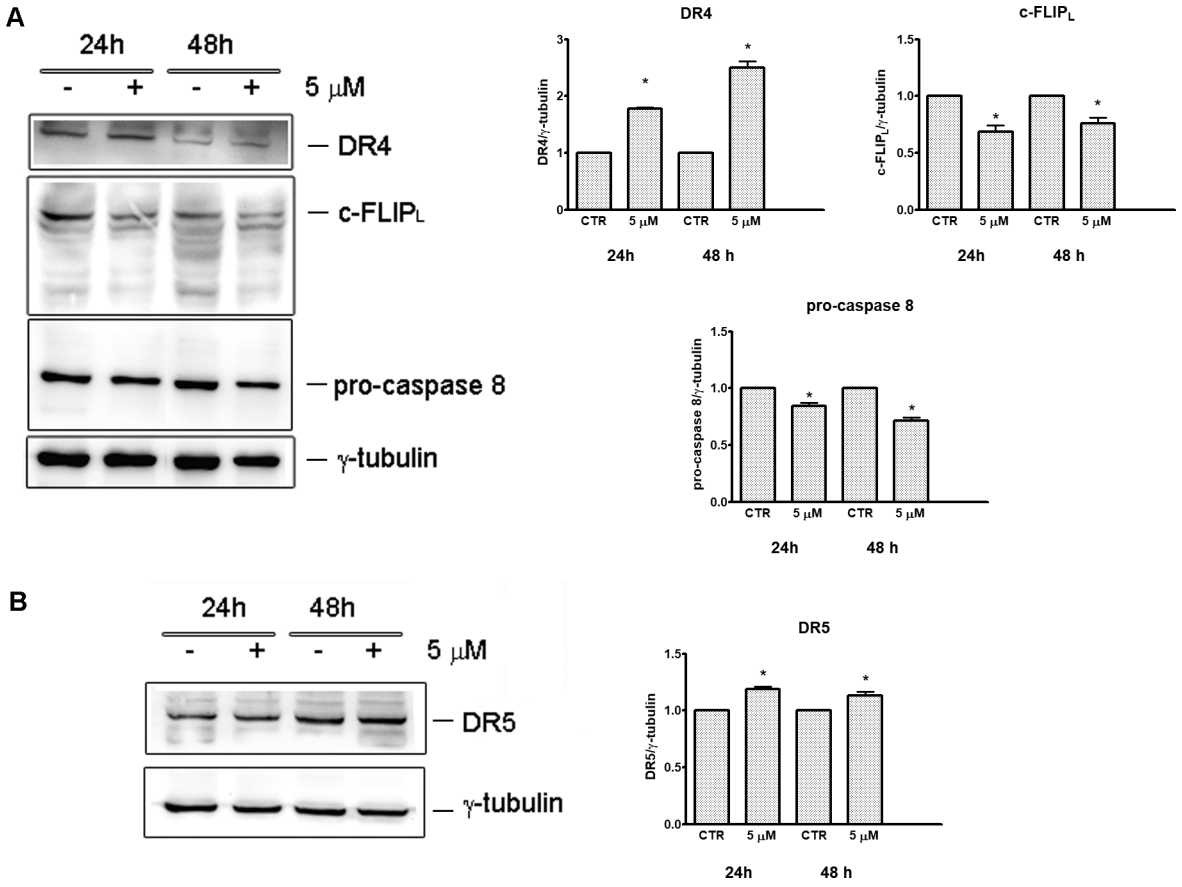

Fig. 9. Western blotting analyses of death receptor-mediated pathway in **26c**-treated H292 cells. DR4, DR5, c-FLIP and pro-caspase 8 analyses were performed after 24 and 48 h of treatment with **26c** compound. The correct protein loading was ascertained by immunoblotting for γ-tubulin. Representative blots of three independent experiments and densitometric analysis are shown. (*) $p < 0.05$ compared to the untreated sample.

4. Experimental

4.1. Chemistry

4.1.1. General

Reaction progress was monitored by TLC on silica gel plates (Merck 60, F_{254}, 0.2 mm). Organic solutions were dried over Na_2SO_4. Evaporation refers to the removal of solvent on a rotary evaporator under reduced pressure. All melting points were determined on a Büchi 530 capillary melting point apparatus and are uncorrected. 1H NMR (300 MHz) and 13C NMR (75 MHz) spectra were recorded with a Bruker AC-E spectrometer at r.t.; chemical shifts (δ) are expressed as ppm values. Microanalyses data (C, H, N) were obtained by an Elemental Vario EL III apparatus and were within ± 0.4% of the theoretical values. Yields refer to purified products and are not optimized. The names of the compounds were obtained using Chem Draw Ultra 12.0 software (CambridgeSoft).

4.1.2. General procedure for preparation of 2-nitrobenzoyl chlorides (**25a-c**) [25]

The 3-phenylpropanoyl, 2-phenoxyacetyl and cinnamoyl chlorides **25a-c**, were obtained by refluxing for 5 h the appropriate acid derivatives **24a-c** (0.01 mol) with thionyl chloride (7.25 ml). After evaporation under reduced pressure, the crude liquid residue was used for subsequent reactions without purification.

4.1.3. Preparation of ethyl 5-(4-nitrobenzamido)-1-phenyl-1H-pyrazole-4-carboxylate (**22a**) and ethyl 5-(4-nitrobenzamido)-1-(pyridin-2-yl)-1H-pyrazole-4-carboxylate (**22b**)

Compounds **22a,b** were obtained following a method previously described by us [38]. Equimolar amounts of 4-nitrobenzoyl chloride **20** (3 mmol, 0.56 g) and ethyl 5-amino-1-phenyl-1H-pyrazole-4-carboxylate **21a** or ethyl 5-amino-1-(pyridin-2-yl)-1H-pyrazole-4-carboxylate **21b** or 1H-indazole-6amine **28**, (3 mmol) are dissolved in 10 ml of acetonitrile and placed under reflux for 8 h. After this time, the solution is evaporated under reduced pressure to give a solid which is crystallized from ethanol.

*4.1.3.1. Ethyl 5-(4-nitrobenzamido)-1-phenyl-1H-pyrazole-4-carboxylate (**22a**).* 11% yield, mp 154–156 °C; 1H NMR ($CDCl_3$) δ: 1.37 (t, 3H, CH_3), 4.34 (q, 2H, CH_2), 7.36–8.31 (m, 10H, ArH and pyrazole-H), 9.46 (s, 1H, NH). 13C NMR(δ) ($CDCl_3$) 14.34, 60.84, 106.10, 123.09, 124.06, 128.42, 128.88, 129.27, 137.99, 139.46, 139.86, 140.53, 159.29, 163.08, 164.03. Anal. Calcd. for $C_{19}H_{16}N_4O_5$: C, 60.00%; H, 4.24%; N, 17.73%; Found: C, 59.93%; H, 4.17%; N, 14.63.

*4.1.3.2. Ethyl 5-(4-nitrobenzamido)-1-(pyridin-2-yl)-1H-pyrazole-4-carboxylate (**22b**).* 43% yield, mp 139–140 °C; 1H NMR (DMSO) δ: 1.20 (t, 3H, CH_3), 4.21 (q, 2H, CH_2), 7.42–8.47 (m, 9H, ArH and pyrazole-H), 11.22 (s, 1H, NH). 13C NMR(δ) (DMSO) 15.47, 61.36, 111.42, 118.32, 124.79, 125.21, 130.60, 139.50, 140.12, 140.93, 142.92, 149.49, 150.92, 152.79, 162.84, 165.24. Anal. Calcd. for $C_{18}H_{15}N_5O_5$: C, 56.69%; H, 3.96%; N, 18.37%; Found: C, 56.60%; H, 3.90%; N, 18.44.

4.1.4. Preparation of ethyl 5-(4-aminobenzamido)-1-phenyl-1H-pyrazole-4-carboxylate (**23a**) and ethyl 5-(4-aminobenzamido)-1-(pyridin-2-yl)-1H-pyrazole-4-carboxylate (**23b**)

To a solution of 1.3 mmol of compound **22a,b** in 75 ml of warm ethanol, 100 mg of 10% Pd-C as catalyst was added. The mixture was

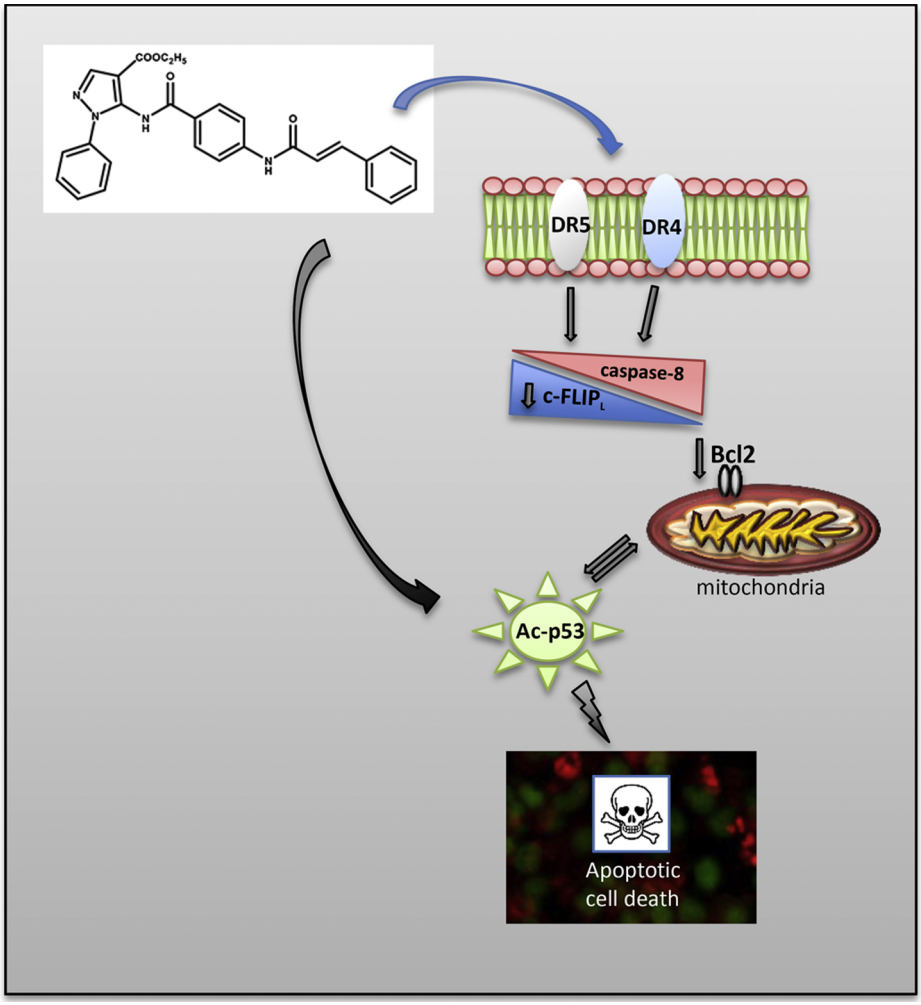

Fig. 10. Schematic representation of **26c** effect in H292 cells. **26c** induces intrinsic apoptotic pathway by activating p53. Moreover, the compound is able to activate TRAIL-inducing pathway by promoting activation of DR4 and DR5 death receptors, downregulation of c-FLIP$_L$ and caspase-8 activation. Both intrinsic and extrinsic pathway may be responsible for Bcl-2 down-regulation and activation of executioner caspases.

left under hydrogenation in a Parr apparatus at 50 psi for 20 h. The suspension was filtered and the filtrate was evaporated affording the crude compound **23a,b** which was crystallized from ethanol.

*4.1.4.1. Ethyl 5-(4-aminobenzamido)-1-phenyl-1H-pyrazole-4-carboxylate **(23a)***. 83% yield, mp 105–106 °C; 1H NMR ($CDCl_3$) δ: 1.34 (t, 3H, CH_3); 4.12 (s, 2H, NH_2); 4.30 (q, 2H, CH_2); 6.59–7.67 (m, 10H, ArH and pyrazole-H); 9.20 (s, 1H, NH). 13C NMR(δ) ($CDCl_3$) 14.36, 60.48, 104.93, 114.07, 121.75, 122.88, 127.84, 129.08, 129.80, 140.36, 140.49, 140.81, 150.91, 164.13, 164.59. Anal. Calcd. for $C_{19}H_{18}N_4O_3$: C, 65.13%; H, 5.18%; N, 15.99%; Found: C, 64.73%; H, 4.97%; N, 16.19.

*4.1.4.2. Ethyl 5-(4-aminobenzamido)-1-(pyridin-2-yl)-1H-pyrazole-4-carboxylate **(23b)***. 49% yield, mp 185–187 °C; 1H NMR (DMSO) δ: 1.17 (t, 3H, CH_3), 4.17 (q, 2H, CH_2), 5.93 (s, 2H, NH_2), 6.59–8.49 (m, 9H, ArH and pyrazole-H); 10.58 (s, 1H, NH). 13C NMR(δ) (DMSO) 15.49, 61.08, 109.83, 114.05, 118.15, 120.56, 124.41, 131.00, 140.90, 141.22, 142.73, 149.29, 153.25, 154.22, 163.26, 165.59. Anal. Calcd. for $C_{18}H_{17}N_5O_3$: C, 61.53%; H, 4.88%; N, 19.93%; Found: C, 61.55%; H, 4.90%; N, 19.77.

*4.1.5. General procedure [38] for preparation of compounds **(26a-c)** and **(27a-c)***

An equimolar amount of ethyl 5-(4-aminobenzamido)-1-phenyl-1H-pyrazole-4-carboxylate **23a** or ethyl 5-(4-aminobenzamido)-1-(pyridin-2-yl)-1H-pyrazole-4-carboxylate **23b** (1.425 mmol) and the appropriate benzoyl chloride **25a-c** (1.425 mmol) in acetonitrile (5 ml) was refluxed for 8 h. The solvent was evaporated under reduced pressure and the residue filtered and recrystallized from ethanol.

*4.1.5.1. Ethyl 1-phenyl-5-(4-(3-phenylpropanamido)benzamido)-1H-pyrazole-4-carboxylate **(26a)***. 52% yield, mp 200–202 °C; 1H NMR ($CDCl_3$) δ: 1.33 (t, 3H, CH_3); 2.62 (t, 2H, CH_2); 3.01 (t, 2H, CH_2); 4.30 (q, 2H, CH_2); 7.17–8.01 (m, 15H, ArH and pyrazole-H); 8.03 (s, 1H, NH); 9.23 (s, 1H, NH). 13C NMR(δ) ($CDCl_3$) 14.35, 31.34, 39.39, 60.59, 105.46, 119.31, 122.96, 126.50, 127.74, 128.08, 128.35, 128.70, 128.86, 129.15, 140.08, 140.13, 140.35, 140.57, 141.97, 163.94, 164.31, 170.70. Anal. Calcd. for $C_{28}H_{26}N_4O_4$: C, 69.70%; H, 5.43%; N, 11.61%; Found: C, 69.66%; H, 5.62%; N, 11.81.

*4.1.5.2. Ethyl 5-(4-(2-phenoxyacetamido)benzamido)-1-phenyl-1H-pyrazole-4-carboxylate **(26b)***. 56% yield, mp 182–184 °C; 1H NMR ($CDCl_3$) δ: 1.34 (t, 3H, CH_3); 4.31 (q, 2H, CH_2); 4.61 (s, 2H, OCH_2); 6.97–8.02 (m, 15H, ArH and pyrazole-H); 8.49 (s, 1H, NH), 9.31 (s, 1H, NH). 13C NMR(δ) ($CDCl_3$) 14.37, 60.63, 67.55, 76.83, 105.44, 114.84, 119.66, 122.69, 122.98, 128.11, 128.52, 129.04, 129.18, 129.99, 140.08, 140.58, 140.89, 156.79, 163.97, 164.17, 166.66. Anal. Calcd. for $C_{27}H_{24}N_4O_5$: C, 66.93%; H, 4.99%; N, 11.56%; Found: C, 66.93%; H, 5.23%; N, 11.81.

*4.1.5.3. Ethyl 5-(4-cinnamamidobenzamido)-1-phenyl-1H-pyrazole-4-carboxylate (**26c**)*. 24% yield, mp 203–205 °C; 1H NMR (DMSO) δ: 1.39 (t, 3H, CH_3); 4.17 (q, 2H, CH_2); 6.86 (d, 1H, J = 15.9 Hz, olefinic-H); 7.43–7.92 (m, 15H, ArH and olefinic-H); 8.18 (s, 1H, pyrazole-H); 10.39 (s, 1H, NH); 10.55 (s, 1H, NH). 13C NMR(δ) ($CDCl_3$) 14.56, 60.24, 110.16, 119.04, 122.30, 124.20, 127.76, 128.31, 128.89, 129.34, 129.53, 129.73, 130.48, 135.01, 138.38, 139.20, 141.45, 141.76, 143.32, 162.03, 164.42, 166.43. Anal. Calcd. for $C_{28}H_{24}N_4O_4$: C, 69.99%; H, 5.03%; N, 11.66%; Found: C, 69.82%; H, 5.43%; N, 12.06.

*4.1.5.4. Ethyl 5-(4-(3-phenylpropanamido)benzamido)-1-(pyridin-2-yl)-1H-pyrazole-4-carboxylate (**27a**)*. 73% yield, mp 137–138 °C; 1H NMR ($CDCl_3$) δ: 1.28 (t, 3H, CH_3); 2.68 (t, 2H, CH_2); 3.02 (t, 2H, CH_2); 4.29 (q, 2H, CH_2); 7.18–8.02 (m, 13H, ArH and pyrazole-H); 8.24 (s, 1H, NH); 8.38 (d, 1H, ArH); 11.32 (s, 1H). 13C NMR(δ) ($CDCl_3$) 14.31, 31.35, 39.25, 60.70, 107.43, 116.72, 119.33, 122.49, 126.35, 127.71, 128.39, 128.61, 128.94, 140.26, 140.58, 140.75, 142.26, 142.34, 145.88, 152.20, 162.96, 163.44, 171.14. Anal. Calcd. for $C_{27}H_{25}N_5O_4$: C, 67.07%; H, 5.21%; N, 14.48%;. Found: C, 67.30%; H, 4.82%; N, 14.43.

*4.1.5.5. Ethyl 5-(4-(2-phenoxyacetamido)benzamido)-1-(pyridin-2-yl)-1H-pyrazole-4-carboxylate (**27b**)*. 48% yield, mp 173–174 °C; 1H NMR ($CDCl_3$) δ: 1.29 (t, 3H, CH_3); 4.31 (q, 2H, CH_2); 4.63 (s, 2H, OCH_2); 6.98–8.39 (m, 14H, ArH and pyrazole-H); 8.58 (s, 1H, NH), 11.51 (s, 1H, NH). 13C NMR(δ) ($CDCl_3$) 14.34, 60.49, 67.54, 107.51, 114.81, 115.82, 119.70, 122.02, 122.62, 129.10, 129.28, 129.97, 139.54, 139.79, 140.77, 141.96, 146.89, 153.38, 156.82, 162.91, 162.98, 166.68. Anal. Calcd. for $C_{26}H_{23}N_5O_5$: C, 64.32%; H, 4.78%; N, 14.43%; Found: C, 64.65%; H, 4.68%; N, 14.57.

*4.1.5.6. Ethyl 5-(4-cinnamamidobenzamido)-1-(pyridin-2-yl)-1H-pyrazole-4-carboxylate (**27c**)*. 15% yield, mp 204–206 °C; 1H NMR (DMSO) δ: 1.20 (t, 3H, CH_3); 4.21 (q, 2H, CH_2); 6.90 (d, 1H, J = 15.6 Hz, olefinic-H); 7.45–8.50 (m, 15H, ArH, pyrazole-H and olefinic-H); 10.59 (s, 1H, NH); 10.87 (s, 1H, NH). 13C NMR(δ) (DMSO) 14.60, 60.29, 109.80, 117.40, 119.12, 122.23, 123.71, 128.02, 128.32, 129.38, 129.52, 130.46, 135.03, 139.59, 139.99, 141.43, 141.94, 143.32, 148.54, 152.14, 162.15, 164.43, 164.76. Anal. Calcd. for $C_{27}H_{23}N_5O_4$: C, 67.35%; H, 4.81%; N, 14.54%; Found: C, 67.42%; H, 4.62%; N, 14.83.

*4.1.6. Preparation [39] of N-(1H-indazol-6-yl)-4-nitrobenzamide (**29**)*

To a stirred cold (ice bath, 0–5 °C) solution of 1H-indazole-6-amine **28** (611 mg, 5.4 mmol) in pyridine (16 ml), 4-nitro-benzoyl chloride **20** (1 g, 5.4 mmol) was added dropwise. Stirring was continued for 24 h then the white slurry was poured into crushed ice. The solid that separated out was filtered off and recrystallized from ethanol to give pure **29**.

*4.1.6.1. N-(1H-Indazol-6-yl)-4-nitrobenzamide (**29**)*. 58% yield, mp > 250 °C; 1H NMR ($CDCl_3$) δ: 8.39–7.39 (m, 8H, ArH); 10.71 (s, 1H, NH); 13.03 (s, 1H, indazole-H). Anal. Calcd. for $C_{14}H_{10}N_4O_3$: C, 59.57%; H, 3.57%; N, 19.85%; Found: C, 59.82%; H, 3.85%; N, 19.83.

*4.1.7. Preparation of N-(1H-indazol-6-yl)-4-aminobenzamide (**30**)*

Compound **30** was obtained with the same method used for the compounds **23a,b** solubilizing the nitro compound **29** (880 mg, 3.12 mmol) in warm ethanol (mL 120) adding 88 mg of 10% Pd-C as catalyst.

*4.1.7.1. N-(1H-Indazol-6-yl)-4-aminobenzamide (**30**)*. 42% yield, mp > 250 °C; 1H NMR (DMSO) δ: 5.82 (s, 2H, NH_2); 6.64–7.98 (m, 7H, ArH); 8.30 (s, 1H, indazole-H); 9.95 (s, 1H, NH), 12.95 (s, 1H, indazole NH). 13C NMR(δ) (DMSO) 99.88, 112.87, 115.46, 119.28, 120.51, 121.44, 129.72, 133.52, 138.29, 140.73, 152.46), 165.91. Anal. Calcd. for $C_{14}H_{12}N_4O$: C, 66.65%; H, 4.79%; N, 22.21%; Found: C, 67.01%; H, 4.90%; N, 22.13.

*4.1.8. General procedure [39] for preparation of compounds (**31a,b**)*

To a stirred cold (ice bath, 0–5 °C) solution of N-(1H-indazol-6-yl)-4-aminobenzamide **30** (400 mg, 1.6 mmol) in pyridine (1.3 ml), the appropriate benzoyl chloride **25a-c** (1.6 mmol) was added dropwise. Stirring was continued for 24 h then the white slurry was poured into crushed ice. The solid that separated out was filtered off and recrystallized to give pure **31a,b**.

*4.1.8.1. N-(1H-Indazol-6-yl)-4-(3-phenylpropanamido)benzamide (**31a**)*. 63% yield, mp > 250 °C (ethyl acetate); 1H NMR (DMSO) δ: 2.68 (t, 2H, CH_2); 2.93 (t, 2H, CH_2); 7.19–8.26 (m, 13H, ArH and indazole-H); 10.22 (s, H, NH); 10.23 (s, H, NH); 12.95 (s, 1H, indazole-NH). 13C NMR(δ) (DMSO) 31.15, 38.51, 100.38, 115.55, 118.63, 119.77, 120.82, 126.50, 128.71, 128.80, 129.11, 129.63, 133.76, 137.92, 140.75, 141.55, 142.63, 165.89, 171.60. Anal. Calcd. for $C_{23}H_{20}N_4O_2$: C, 71.86%; H, 5.24%; N, 14.57%; Found: C, 72.02%; H, 5.18%; N, 14.57.

*4.1.8.2. N-(1H-Indazol-6-yl)-4-(2-phenoxyacetamido)benzamide (**31b**)*. 95% yield, mp > 250 °C; 1H NMR ($CDCl_3$) δ: 4.76 (s, 2H, OCH_2); 7.02–8.27 (m, 13H, ArH); 10.29 (s, 1H, NH), 10.43 (s, 1H, NH), 12.97 (s, 1H, indazole-NH). 13C NMR(δ) ($CDCl_3$) 68.39, 101.32, 116.01, 116.45, 120.21, 120.68, 121.77, 122.60, 130.04, 130.92, 131.12, 134.66, 138.82, 141.65, 142.75, 159.13, 166.49, 168.46. Anal. Calcd. for $C_{22}H_{18}N_4O_3$: C, 68.38%; H, 4.70%; N, 14.50%; Found: C, 68.73%; H, 4.47%; N, 14.17.

*4.1.9. Procedure for preparation of 4-nitro-N-(1-(4-nitrobenzoyl)-1H-indazol-3-yl)benzamide (**34**)*

Attempt to obtain the N-(1H-indazol-3-yl)-4-nitrobenzamide **33** (Scheme 3) with the same method [38] used for compound **29** failed. Immediately a precipitate is formed which appears to be the 4-nitro-N-(1-(4-nitrobenzoyl)-1H-indazol-3-yl)benzamide **34**.

*4.1.9.1. 4-Nitro-N-(1-(4-nitrobenzoyl)-1H-indazol-3-yl)benzamide (**34**)*. 73% yield, mp 222–225 °C; 1H NMR (DMSO) δ: 7.47–8.49 (m, 12H, ArH); 11.67 (s, 1H, NH). 13C NMR(δ) (DMSO) 115.80, 121.28, 123.46, 123.77, 124.02, 125.47, 130.25, 130.96, 132.09, 139.17, 139.60, 140.71, 146.83, 149.55, 150.05, 165.23, 166.30. Anal. Calcd. for $C_{21}H_{13}N_5O_6$: C, 58.47%; H, 3.04%; N, 16.24%; Found: C, 58.32%; H, 2.90%; N, 16.35.

4.2. Biology

4.2.1. Materials and methods

4.2.1.1. Cell culture and treatment conditions. The human lung mucoepidermoid carcinoma H292 cells (American Type Culture Collection, ATCC) and human dermal fibroblasts HDFα (gently provided by Dr Marta Di Carlo) were cultured in RPMI-1640 medium (Sigma Aldrich, Milan, Italy) supplemented with 10% heat-inactivated Fetal Bovine Serum, 100 U/mL streptomycin, and 100 U/mL penicillin (Life Technology, Milan, Italy) in a humidified atmosphere with 5% CO_2, as previously reported [31]. The cells were grown as monolayers attached to 75 cm^2 culture flasks and cultured at 37 °C in a 5% CO_2 humidified incubator.

Synthesized compounds **26a-c**, **27a-c** and **31a,b** were prepared as a 20 mM stock solution in dimethyl sulfoxide (DMSO), stored at 20 °C and freshly dissolved immediately before use. The maximum final concentration of DMSO in the medium was less than 0.01%. Working dilutions were made in sterile medium and added to the complete cell culture medium at the appropriate concentrations. Twenty-four hours after seeding, when the cells reached 70% confluency, the cultures were treated with a range of concentrations of compounds. Cells were

routinely photographed before and after incubation with the compounds to record morphological changes occurring in the cells, using an inverted light microscope equipped with phase contrast rings (LEICA DM-IRB, Leica Microsystem, Milan, Italy).

4.2.1.2. MTT assay. The viability of both lung mucoepidermoid carcinoma H292 cells and human dermal fibroblasts HDFα treated with compounds **26a-c**, **27a-c** and **31a,b** was measured using 3-(4,5-dimethylthiazol-2-yl)-2,3-diphenyltetrazolium bromide (MTT) colorimetric assay. Briefly, 5×10^3 cells were plated in 200 µl of complete medium per well in 96-well plates and treated with various concentrations of compounds. Then, cell viability analysis by MTT was performed as described [40]. MTT is reduced to purple formazan in the mitochondria of living cells. The absorbance of the formazan was measured at 570 nm, with 630 nm as a reference wavelength by scanning the relative cell viability with an ELISA plate reader (OPSYS MR, Dynex Technologies).

Cell viability was expressed as the percentage of the OD value of inhibitor-treated cells compared with untreated samples used as control. Each experiment was performed in triplicate.

4.2.1.3. Clonogenic assay. The single cells were seeded in RPMI 1640 with 10% FBS at a density of 200 cells/well on 6-well plates. After 10 days, the colony formation ability was assessed by counting the number of colonies under a microscope after crystal violet staining (Sigma-Aldrich, St. Louis, MO, USA). Briefly, medium was removed and cells were washed in cold PBS and then incubated on ice in cold methanol for 15 min. Thereafter, cells were washed in PBS, incubated for 1 h in the presence of 0.01% crystal violet. Representative views were photographed.

4.2.1.4. Assessment of apoptotic cell death and cell cycle distribution. The apoptotic morphology was analyzed by acridine orange and ethidium bromide (AO/EO) staining solution (100 µg/ml PBS of each dye), a combination of fluorescent DNA binding dyes [41].

For these studies, H292 cells were seeded into 96-well plates, treated with compounds for the indicated times at 37 °C. Thereafter, the incubation medium was removed, cells were washed with PBS and then incubated with AO/EO staining solution. All conditions were analyzed by a Leica DM IRB inverted microscope (Leica Microsystems Srl) equipped with fluorescence optics and suitable filters for FITC and rhodamine detection; images were captured by a computer-imaging system (Leica DC300F camera for image analysis) using the Leica Q Fluoro Software.

Apoptosis was also studied by flow cytometry analysis [35]. For these studies, cell pellets were washed 3 times with PBS and re-suspended at 1×10^6 cells/ml in propidium iodide (PI) staining solution (3.8 mM sodium citrate, 25 µg/ml PI, 10 µg/ml RNase A; Sigma-Aldrich) and kept for 3 h at 4 °C in the dark prior to flow cytometry analysis performed by a FACscan (Becton Dickinson, San Diego, CA). The proportion of cells in the sub-G0/G1 peak of cell cycle was taken as a measure of apoptotic cell death.

4.2.1.5. Western blotting analysis. For these studies, after treatment, cells were washed in PBS and lysed for 30 min at 4 °C in ice-cold lysis buffer (1% NP40, 0.1% SDS, and 0.5% sodium deoxycolate in PBS) containing protease inhibitor cocktail. Then, cells were sonicated three times for 10 s and protein content was assayed using Bradford method (Bio-Rad Laboratories) as previously reported [42]. Equal amounts of proteins (40 µg/lane) were resolved on SDS-PAGE gels, transferred on a nitrocellulose membrane (Bio-Rad Laboratories Srl) for the detection with specific antibodies anti-p53, anti-acetyl p53 (Lys 373–382); anti-Bcl-2; anti-DR4; anti-DR5; anti c-FLIP$_L$; anti-pro-caspase-8; anti-γ-tubulin.

Unless otherwise specified all antibodies (diluted 1:250) were purchased from Santa Cruz Biotechnology. All secondary horseradish peroxidase-labeled antibodies were purchased from Amersham Life Science Inc. Immunoreactive signals were detected using enhanced chemiluminescence (ECL) reagents (Bio-Rad). The correct protein loading was confirmed by stripping the immunoblot and reprobing with primary antibody for γ-tubulin (diluted 1:5000; Sigma).

4.2.1.6. Statistical analysis. The statistical analysis of data was performed using the GraphPad Prism 5 software package (San Diego, CA). The data obtained were compared by the One-way ANOVA analysis of variance using Bonferroni post-hoc multiple comparisons. The data are expressed as means ± SD. The statistical significance threshold was fixed at $p < 0.05$.

Acknowledgement

Financial support from “Fondo di Finanziamento della Ricerca di Ateneo, University of Palermo” is gratefully acknowledged.

References

[1] D.W. Meek, Biochem. J. 469 (2015) 325–346, https://doi.org/10.1042/BJ20150517.
[2] D.W. Meek, C.W., Cold Spring Harb. Perspect. Biol. 1 (2009) a000950-a000950. http://doi.org/10.1101/cshperspect.a000950.
[3] A. Sancar, L.A. Lindsey-Boltz, K. Ünsal-Kaçmaz, S. Linn, Annu. Rev. Biochem. 73 (2004) 39–85, https://doi.org/10.1146/annurev.biochem.73.011303.073723.
[4] A. Marino Gammazza, C. Campanella, R. Barone, C. Caruso Bavisotto, M. Gorska, M. Wozniak, F. Carini, F. Cappello, A. D'Anneo, M. Lauricella, G. Zummo, E. Conway de Macario, A.J.L. Macario, V. Di Felice, Cancer Lett. 385 (2017) 75–86, https://doi.org/10.1016/j.canlet.2016.10.045.
[5] Y. Wang, J. Zhong, J. Bai, R. Tonga, F. An, P. Jiao, L. He, D. Zeng, E. Long, J. Yan, J. Yan, L. Cai, Curr. Drug Metab. (1969) (accessed July 25, 2018).
[6] J.-P. Kruse, W. Gu, Cell 137 (2009) 609–622, https://doi.org/10.1016/j.cell.2009.04.050.
[7] H. Shen, C.G. Maki, Curr. Pharm. Des. (2011) (accessed July 25, 2018).
[8] C.J. Brown, S. Lain, C.S. Verma, A.R. Fersht, D.P. Lane, Nat. Rev. Cancer 9 (2009) 862–873, https://doi.org/10.1038/nrc2763.
[9] X. Yu, S. Narayanan, A. Vazquez, D.R. Carpizo, Apoptosis 19 (2014) 1055–1068, https://doi.org/10.1007/s10495-014-0990-3.
[10] S. Zheng, X.Y. Koh, H.C. Goh, S.A.B. Rahmat, L.-A. Hwang, D.P. Lane, Cancer Res. 77 (2017) 4342–4354, https://doi.org/10.1158/0008-5472.CAN-17-0424.
[11] M.C. Bagley, T. Davis, P.G.S. Murziani, C.S. Widdowson, D. Kipling, Pharmaceuticals 3 (2010) 1842–1872, https://doi.org/10.3390/ph3061842.
[12] A. Cuenda, S. Rousseau, Biochim. Biophys. Acta BBA – Mol. Cell Res. 1773 (2007) 1358–1375, https://doi.org/10.1016/j.bbamcr.2007.03.010.
[13] M.J.G.W. Ladds, I.M.M. van Leeuwen, C.J. Drummond, S. Chu, A.R. Healy, G. Popova, A. Pastor Fernández, T. Mollick, S. Darekar, S.K. Sedimbi, M. Nekulova, M.C.C. Sachweh, J. Campbell, M. Higgins, C. Tuck, M. Popa, M.M. Safont, P. Gelebart, Z. Fandalyuk, A.M. Thompson, R. Svensson, A.-L. Gustavsson, L. Johansson, K. Färnegårdh, U. Yngve, A. Saleh, M. Haraldsson, A.C.A. D'Hollander, M. Franco, Y. Zhao, M. Håkansson, B. Walse, K. Larsson, E.M. Peat, V. Pelechano, J. Lunec, B. Vojtesek, M. Carmena, W.C. Earnshaw, A.R. McCarthy, N.J. Westwood, M. Arsenian-Henriksson, D.P. Lane, R. Bhatia, E. McCormack, S. Laín, Nat. Commun. 9 (2018), https://doi.org/10.1038/s41467-018-03441-3.
[14] Z.-Q. Ning, Z.-B. Li, M.J. Newman, S. Shan, X.-H. Wang, D.-S. Pan, J. Zhang, M. Dong, X. Du, X.-P. Lu, Cancer Chemother. Pharmacol. 69 (2012) 901–909, https://doi.org/10.1007/s00280-011-1766-x.
[15] R.R. Rosato, J.A. Almenara, S. Grant, Cancer Res. 63 (2003) 3637–3645.
[16] S. Lain, J.J. Hollick, J. Campbell, O.D. Staples, M. Higgins, M. Aoubala, A. McCarthy, V. Appleyard, K.E. Murray, L. Baker, A. Thompson, J. Mathers, S.J. Holland, M.J.R. Stark, G. Pass, J. Woods, D.P. Lane, N.J. Westwood, Cancer Cell 13 (2008) 454–463, https://doi.org/10.1016/j.ccr.2008.03.004.
[17] G. BoijeafGennäs, L. Mologni, S. Ahmed, M. Rajaratnam, O. Marin, N. Lindholm, M. Viltadi, C. Gambacorti-Passerini, L. Scapozza, J. Yli-Kauhaluoma, ChemMedChem 6 (2011) 1680–1692, https://doi.org/10.1002/cmdc.201100168.
[18] Y.H.E. Mohammed, V.H. Malojirao, P. Thirusangu, M. Al-Ghorbani, B.T. Prabhakar, S.A. Khanum, Eur. J. Med. Chem. 143 (2018) 1826–1839, https://doi.org/10.1016/j.ejmech.2017.10.082.
[19] B. Maggio, M.V. Raimondi, D. Raffa, F. Plescia, M.-C. Scherrmann, N. Prosa, M. Lauricella, A. D'Anneo, G. Daidone, Eur. J. Med. Chem. 122 (2016) 247–256, https://doi.org/10.1016/j.ejmech.2016.06.027.
[20] B. Maggio, M.V. Raimondi, D. Raffa, F. Plescia, S. Cascioferro, G. Cancemi, M. Tolomeo, S. Grimaudo, G. Daidone, Eur. J. Med. Chem. 96 (2015) 98–104, https://doi.org/10.1016/j.ejmech.2015.04.004.
[21] B. Maggio, D. Raffa, M.V. Raimondi, M.G. Cusimano, F. Plescia, S. Cascioferro, G. Cancemi, M. Lauricella, D. Carlisi, G. Daidone, Eur. J. Med. Chem. 72 (2014) 1–9, https://doi.org/10.1016/j.ejmech.2013.11.016.
[22] B. Maggio, M.V. Raimondi, D. Raffa, F. Plescia, S. Cascioferro, S. Plescia, M. Tolomeo, A. Di Cristina, R.M. Pipitone, S. Grimaudo, G. Daidone, Eur. J. Med.

Chem. 46 (2011) 168–174, https://doi.org/10.1016/j.ejmech.2010.10.032.
[23] D. Raffa, B. Maggio, S. Cascioferro, M.V. Raimondi, G. Daidone, S. Plescia, D. Schillaci, M.G. Cusimano, L. Titone, C. Colomba, M. Tolomeo, Arch. Pharm. (Weinheim) 342 (2009) 265–273, https://doi.org/10.1002/ardp.200800159.
[24] B. Maggio, D. Raffa, M.V. Raimondi, S. Cascioferro, F. Plescia, M. Tolomeo, E. Barbusca, G. Cannizzo, S. Mancuso, G. Daidone, Eur. J. Med. Chem. 43 (2008) 2386–2394, https://doi.org/10.1016/j.ejmech.2008.01.007.
[25] D. Raffa, F. Plescia, B. Maggio, M.V. Raimondi, A. D'Anneo, M. Lauricella, G. Daidone, Eur. J. Med. Chem. 132 (2017) 262–273, https://doi.org/10.1016/j.ejmech.2017.03.051.
[26] D. Raffa, B. Maggio, F. Plescia, S. Cascioferro, M.V. Raimondi, G. Cancemi, A. D'Anneo, M. Lauricella, M.G. Cusimano, R. Bai, E. Hamel, G. Daidone, Bioorg. Med. Chem. 23 (2015) 6305–6316, https://doi.org/10.1016/j.bmc.2015.08.027.
[27] D. Raffa, B. Maggio, M.V. Raimondi, M.G. Cusimano, G. Amico, A. Carollo, P.G. Conaldi, R. Bai, E. Hamel, G. Daidone, Eur. J. Med. Chem. 65 (2013) 427–435, https://doi.org/10.1016/j.ejmech.2013.04.068.
[28] D. Raffa, B. Maggio, F. Plescia, S. Cascioferro, S. Plescia, M.V. Raimondi, G. Daidone, M. Tolomeo, S. Grimaudo, A. Di Cristina, R.M. Pipitone, R. Bai, E. Hamel, Eur. J. Med. Chem. 46 (2011) 2786–2796, https://doi.org/10.1016/j.ejmech.2011.03.067.
[29] D. Carlisi, B. Vassallo, M. Lauricella, S. Emanuele, A. D'Anneo, E. Di Leonardo, P. Di Fazio, R. Vento, G. Tesoriere, Int. J. Oncol. 32 (2008) 177–184, https://doi.org/10.3892/ijo.32.1.177.
[30] V. Santini, A. Gozzini, G. Ferrari, Curr. Drug Metab. 8 (2007) 383–393, https://doi.org/10.2174/138920007780655397.
[31] C. Campanella, A. D'Anneo, A.M. Gammazza, C.C. Bavisotto, R. Barone, S. Emanuele, F.L. Cascio, E. Mocciaro, S. Fais, E.C.D. Macario, A.J.L. Macario, F. Cappello, M. Lauricella, Oncotarget 7 (2015) 28849–28867, https://doi.org/10.18632/oncotarget.6680.
[32] K.H. Vousden, D.P. Lane, Nat. Rev. Mol. Cell Biol. 8 (2007) 275–283, https://doi.org/10.1038/nrm2147.
[33] C.L. Brooks, W. Gu, Protein Cell 2 (2011) 456–462, https://doi.org/10.1007/s13238-011-1063-9.
[34] X. Li, X. Miao, H. Wang, Z. Xu, B. Li, X. Li, X. Miao, H. Wang, Z. Xu, B. Li, Oncotarget 6 (2015) 35699–35709, https://doi.org/10.18632/oncotarget.5372.
[35] M. Lauricella, A. Ciraolo, D. Carlisi, R. Vento, G. Tesoriere, Biochimie 94 (2012) 287–299, https://doi.org/10.1016/j.biochi.2011.06.031.
[36] S. Emanuele, E. Oddo, A. D'Anneo, A. Notaro, G. Calvaruso, M. Lauricella, M. Giuliano, Rendiconti Lincei Sci. Fis. E Nat. 29 (2018) 397–409, https://doi.org/10.1007/s12210-018-0704-9.
[37] R.E. Henry, Z. Andrysik, R. París, M.D. Galbraith, J.M. Espinosa, EMBO J. 31 (2012) 1266–1278, https://doi.org/10.1038/emboj.2011.498.
[38] D. Raffa, O. Migliara, B. Maggio, F. Plescia, S. Cascioferro, M.G. Cusimano, G. Tringali, C. Cannizzaro, F. Plescia, Arch. Pharm. (Weinheim) 343 (2010) 631–638, https://doi.org/10.1002/ardp.200900317.
[39] S. Plescia, D. Raffa, F. Plescia, G. Casula, B. Maggio, G. Daidone, M.V. Raimondi, M.G. Cusimano, G. Bombieri, F. Meneghetti, Arkivoc 2010 (2010) 163, https://doi.org/10.3998/ark.5550190.0011.a14.
[40] A. D'Anneo, D. Carlisi, M. Lauricella, S. Emanuele, R. Di Fiore, R. Vento, G. Tesoriere, J. Cell. Physiol. 228 (2013) 952–967, https://doi.org/10.1002/jcp.24131.
[41] M. Lauricella, G. Calvaruso, M. Carabillò, A. D'Anneo, M. Giuliano, S. Emanuele, R. Vento, G. Tesoriere, FEBS Lett. 499 (2001) 191–197, https://doi.org/10.1016/S0014-5793(01)02553-4.
[42] D. Carlisi, M. Lauricella, A. D'Anneo, G. Buttitta, S. Emanuele, R. di Fiore, R. Martinez, C. Rolfo, R. Vento, G. Tesoriere, J. Cell. Physiol. 230 (2015) 1276–1289, https://doi.org/10.1002/jcp.24863.